Theoretical Notes
Note 368

JUSTIFICATION AND VERIFICATION OF HIGH-ALTITUDE EMP THEORY

PART I

Conrad L. Longmire

June 1986

Contract No: LLNL-9323905

Prepared for: Lawrence Livermore National Laboratory
P. O. Box 808
Livermore, California 94550

Prepared by: MISSION RESEARCH CORPORATION
735 State Street, PO Drawer 719
Santa Barbara, California 93102

TABLE OF CONTENTS

LIST OF ILLUSTRATIONS

SECTION 1
INTRODUCTION

Over the 22 years since the first publication (Ref. 1) of the theory of High-Altitude Electromagnetic Pulse (HEMP), there have been several doubters of the correctness of that theory. On one occasion it was briefly claimed that the HEMP is a much larger pulse than our theory indicates, and is a longitudinal wave rather than transverse. This claim was easily shown to rest on an incorrect application of a standard formula for the fields of a charge moving at relativistic speed. More commonly, it has been claimed that the HEMP is a much smaller pulse than our theory indicates and it has been implied, though not directly stated in writing, that the HEMP has been exaggerated by those who work on it in order to perpetuate their own employment. It could be noted that, in some quarters, the disparagement of HEMP has itself become an occupation. While we have found that no amount of technical reasoning suffices to quiet such criticism, we have learned to live with it, and even to regard it as possibly having some beneficial effects, for example in bringing the question of the HEMP threat to electrical and electronic systems to the attenuation of a wider circle of individuals who have responsibility for those systems.

Thus our principal concern is to convince individuals, with technical backgrounds and open minds, who for various reasons have not been convinced by previously published papers on HEMP theory, that the theory and calculated results are at least approximately correct. One possible difficulty with previous papers (Refs. 1, 2, 3) is that they are based on solving Maxwell's equations. While that is the most legitimate

approach for the mathematically inclined reader, many of the individuals we think it important to reach may not feel comfortable with that approach. We admit to being surprised at the number of people who have wanted to understand HEMP in terms of the fields radiated by individual Compton recoil electrons. Apparently our schools do a better job in teaching the applications of Maxwell's equations (in this case, the cyclotron radiation) than they do in imparting a basic understanding of those equations and how they work. However, the generation of the HEMP can be understood quite well on the basis of concepts familiar to all electrical engineers and physicists. A derivation of the outgoing wave equation based on these concepts is presented in Section 2. This equation, though extremely simple, gives the HEMP to an accuracy of a few percent in practical cases. We also show that adding the fields radiated by individual electrons gives exactly the same answer in a simple but relevant example.

The confidence we have in our calculations of the HEMP rests on two circumstances. The first of these is the basic simplicity of the theory. The physical processes involved, e.g., Compton scattering, are quite well known, and the physical parameters needed in the calculations, such as electron mobility, have been measured in relevant laboratory experiments. There is no mathematical difficulty in determining the solution of the outgoing wave equation, or in understanding why it is an accurate approximation. Nevertheless, to acquire a sufficient understanding of HEMP to be able to say, of one's own knowledge, that our answers are right to 10 or 20% (or wrong) is not a trivial exercise. While the concepts we start with are familiar, in applying them we shall soon come into new ground for many readers. One will not find our problem worked out in textbooks. For example, the model of cyclotron radiation from individual Compton recoil electrons is very difficult to apply with accuracy to our problem because of the multitudinous secondary electrons, which absorb the radiation emitted by the Compton electrons. Readers who

have the patience to follow the development in Section 2 will see that the outgoing wave theory provides a way to avoid unnecessary complications and reduces the problem to its barest essentials.

The other circumstance is that there is experimental data on the HEMP obtained by the Los Alamos Scientific Laboratory in the nuclear test series carried out in 1962. In a classified companion report (Ref. 4) we present calculations of the HEMP from the Kingfish and Bluegill events and compare them with the experimental data. These calculations were performed some years ago, but have not been widely circulated. In order to make the calculations transparently honest, the gamma-ray output was provided by Los Alamos, the HEMP calculations were performed by MRC and the comparison with the experimental data was made by RDA. The degree of agreement between calculation and experiment gives important verification of the correctness of HEMP theory.

A feature of HEMP theory that has troubled some people is that it determines the radiated fields by integrating along the single ray from nuclear burst to observer. The angular derivatives in Maxwell's equations are dropped, which amounts to neglecting diffraction in the propagation of the HEMP. The first paper on HEMP (Ref. 1) contained a justification of this neglection, based on the large ratio of the transverse dimension of the radiating volume compared with the wavelengths in the HEMP. However, we have always wondered just how large a correction diffraction would make for Kingfish, a fairly severe geometry. In Section 3, a method for calculating the effect of diffraction is developed. The method is applied in Reference 4 to that event and the effect is found to be less than 1%. This calculation starts from Maxwell's equations, but we hope that many readers will follow the not-very-complicated mathematics.

Finally, we wish to call attention to two other, unclassified reports that, together with this one, provide a fairly complete explanation of HEMP to readers who may not be experts in mathematical electromagnetic physics. Reference 5 explains details of Compton electron dynamics, secondary electron production and the electric conductivity they make. Reference 6 presents HEMP environments for a large yield nuclear burst at 400 km altitude, shows the wide variability of the HEMP with ground range and azimuth of the observer, and provides analytical formulae fitting the calculated HEMP as a function of range and azimuth. That report also examines in detail the Compton current, air conductivity and fields in the calculation and shows that they are consistent with the relevant physics and the outgoing wave theory. Those two reports and this one should remove all reasonable doubt that our HEMP calculations are at least approximately correct.

SECTION 2
THEORY OF THE GENERATION OF HEMP

2.1 GAMMA RAYS AND COMPTON SCATTERING

Nuclear bombs emit a small fraction, of the order of 0.003, of their energy in gamma rays. Thus a 1-megaton bomb, which produces total energy of about 4.2×10^{15} J (Joules) may emit 3 kilotons or about 1.2×10^{13} J in gamma rays. Gamma rays are electromagnetic waves, like radio waves or visible light, but of much higher frequency than either of these--in the range of 10^{20} to 10^{21} Hz. They travel at the speed of light ($c = 3\times10^{8}$ m/sec), and so have wavelengths of the order of 10^{-10} cm. This is smaller than the diameter of atoms ($\sim10^{-8}$ cm), and in interacting with atoms, gamma rays act more like particles than waves. As a particle, or quantum of electromagnetic radiation, a gamma ray has an energy of the order

$$E_\gamma \approx 2 \text{ MeV} \approx 3.2\times10^{-13} \text{ J} \quad . \tag{1}$$

(The MeV unit of energy is a convenient one in nuclear physics; it is equal to the energy gained by an electron in falling through a potential drop of 10^6 V.) Thus the total number of gammas emitted by a 1 megaton bomb may be of the order

$$N_\gamma \approx 4\times10^{25} \text{ gammas} \quad . \tag{2}$$

The principal interaction of gamma rays with air atoms, or other matter, is Compton scattering. In this process, the gamma collides with an electron in the air atom and knocks it out of the atom. In so doing, the gamma transfers part of its energy (on the average about half) to the electron, and is scattered into a new direction. The Compton recoil electron goes generally near the forward direction of the original gamma, never in backward directions. Thus a directed flux of gammas produces a directed electric current of Compton recoil electrons. This current produces the EMP.

The mean free path for Compton scattering in sea-level air is of the order

$$\lambda_\gamma \approx 180 \text{ m} \quad \text{(at sea level)} \quad . \tag{3}$$

At higher altitudes, where the air density is smaller, λ_γ is correspondingly longer. Since the total mass of air in the atmosphere is about 1000 gm/cm^2, and since the mean free path can also be expressed as

$$\lambda_\gamma = 22 \text{ gm/cm}^2 \quad \text{(at any altitude)} \quad , \tag{4}$$

the total number of mean free paths in the atmosphere for gammas coming vertically downwards is

$$N_\lambda = 1000/22 \approx 45 \quad . \tag{5}$$

Only a very small fraction, $\exp(-N_\lambda) \approx 10^{-20}$, of the gammas reach the ground without being scattered. Most of the gammas will suffer their first scattering near the altitude where they have traversed one mean free path. This is the altitude above which there are 22 gm/cm^2 of air and is about

$$z_s = 30 \text{ km} \quad . \tag{6}$$

Because the air density ρ_a falls approximately exponentially with altitude z,

$$\rho_a \approx \rho_0 \exp(-z/h) \quad , \tag{7}$$

where the scale height h is

$$h \approx 6.7 \text{ km} \quad \text{at 30 km altitude} \quad , \tag{8}$$

the local mean free path at this altitude is approximately equal to h. Thus most of the gammas make their first scattering in a layer of air of thickness h centered about z_s. This is the source region of the HEMP. Scattered gammas make little further contribution to the HEMP, for reasons to be explained below.

We can now calculate the density of Compton electrons in the source region. Let us put our nominal 1-megaton bomb at an altitude of 100 km, 70 km above the source region. Then the number of gammas incident on the source region per unit area, assuming they are emitted isotropically by the bomb, is

$$N_A = N_\gamma/4\pi r^2 = 6.5\times10^{14} \text{ gammas/m}^2 \quad . \tag{9}$$

Since every gamma will make a Compton electron, the number of first-scatter Compton electrons per unit area is also N_A. On the assumption that the gammas are scattered in a height h, the number of birth places of first-scatter Compton electrons per unit volume is

$$N_{bp} = N_A/h = 1.0\times10^{11} \text{ b.p.'s/m}^3 \quad . \tag{10}$$

The density of Compton electrons would be the same as this number if they did not move. Because they move in the same direction as the gammas with an average speed of about 0.9 c, their actual density is about 10 times this number shortly after birth, or about $10^{12}/m^3$. (This point is explained in Section 2.2 below.)

An important question is whether the density of Compton electrons is large enough to justify regarding the current they make as a continuous function. The answer to this question depends on the wavelength of electromagnetic fields that they produce and that are of interest. The duration of the HEMP (or that part of it that is of interest to us) is at least 10^{-8} second, so that wavelengths are a few meters. If we wish to resolve the Compton current on the scale of one quarter of a wavelength, or about 1 meter, we need to consider the number of Compton electrons in a volume of 1 m^3. This is about 10^{12} electrons. The average fluctuation in this number is about $\sqrt{10^{12}} = 10^6$, or 1 part in 10^6. Thus it seems clear that, for the wavelengths of interest, the Compton current density can be quite accurately treated as a continuous function. The coherence of the radiated fields is discussed further in Section 2.3 below.

Note that if the Compton electrons all moved together at nearly the speed of light, they would make a current density

$$J_c \approx 48 \text{ A/m}^2 \quad , \tag{11}$$

a substantial current density.

2.2 THE MOTION OF COMPTON RECOIL ELECTRONS

For 2-MeV gammas, the Compton recoil electrons have an average kinetic energy of about 1 MeV. The most energetic electrons move in the forward direction of the original gamma with kinetic energy 1.78 MeV. The angular distribution of the electrons (per unit solid angle) peaks in the forward direction, and has half of its peak value at about 10° off forward. Thus the Compton electrons are concentrated near the forward direction.

The velocity v of a 1-MeV electron is such that

$$\frac{v}{c} \equiv \beta \approx 0.94 \quad , \tag{12}$$

and the mass is about 3 times its rest mass. In the geomagnetic field appropriate for the central U.S.,

$$B_0 = 0.56 \text{ Gauss} \quad , \tag{13}$$

the gyro (or Larmor) radius of such an electron is

$$L = 85 \text{ m} \quad . \tag{14}$$

The mean stopping range of the 1-MeV electron, due to collisions with electrons in air atoms, at 30 km altitude, is

$$R_m = 170 \text{ m} \quad . \tag{15}$$

This range has been reduced from the extreme range (R_e = 245 m) to account for the multiple scattering of the electron by the nuclei of air atoms. The energy lost by the 1-MeV electron in stopping produces about 30,000

secondary electrons distributed along its path. The secondary electrons have kinetic energies of the order 10 eV at birth. Because their velocities are randomly distributed, they make no significant current of their own accord. However, if an electric field is present, they drift in the direction of the electric force on them, forming an electric conductivity in the air. The conductivity is discussed further in Section 2.4.

Because the mean range of the Compton electron is only about twice its gyro radius, it turns through only about 2 radians or 115° in the geomagnetic field before stopping. Because its mass and gyro radius decrease as it loses energy, it actually turns through a larger angle than this. The average trajectory of the Compton electrons at 30 km altitude will look like that sketched in figure 1.

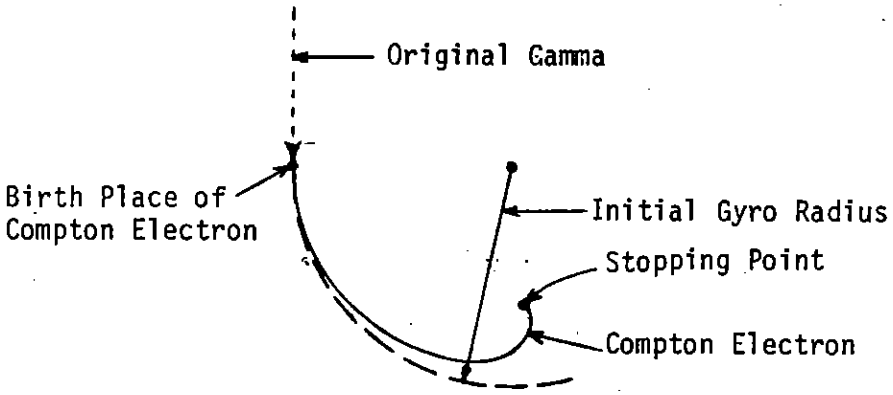

Figure 1. Sketch of average trajectory of Compton electrons from 2-MeV gammas at 30 km altitude.

We can now understand the difference between the density of birth places of Compton electrons and the density of moving Compton electrons. Let us have an impulse function of gammas moving through air. The trajectory of this gamma pulse, i.e., its position r as a function of

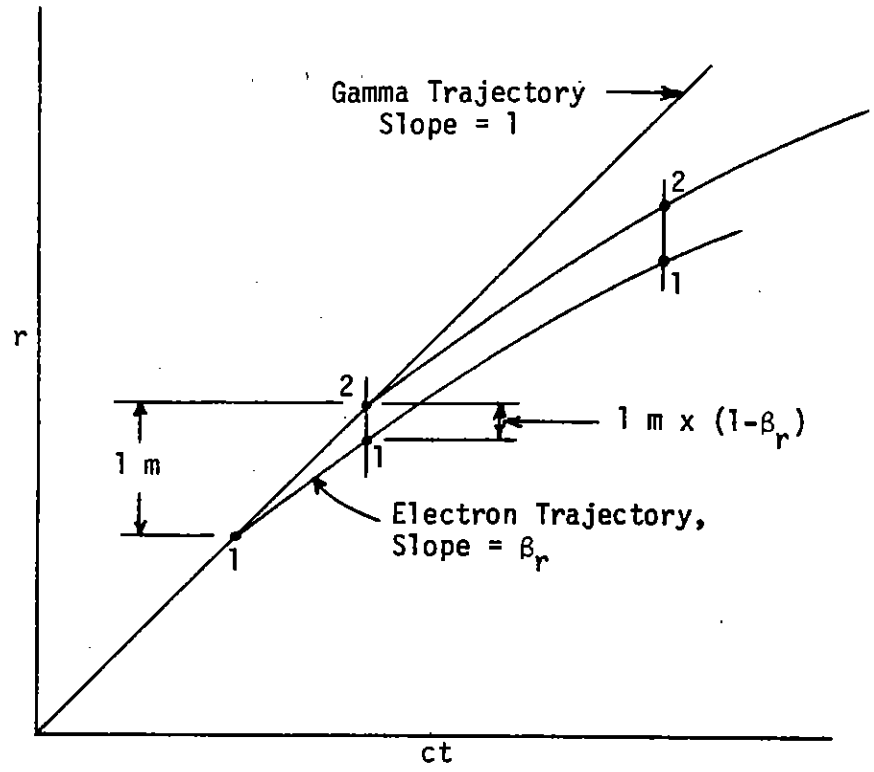

Figure 2. Explanation of motion compression of Compton electrons.

ct (t is time) is indicated in figure 2. Consider also two Compton electrons with birthplaces 1 m apart in r. The trajectories of these electrons, which start with velocity $v_r/c \equiv \beta_r$ slightly less than unity, are identical except that trajectory 2 is translated parallel to the gamma trajectory with respect to that of trajectory 1. The curvature of the electron trajectories is exaggerated in the figure. As indicated in the figure, at the time when the second electron is born, the first electron is a distance 1 m × $(1-\beta_r)$ away from the second. Since all electrons born between 1 and 2 will be in this reduced interval, the relation between the density N_{ce} of Compton electrons and the density N_{bp} of birthplaces is

$$N_{ce} = N_{bp}/(1-\beta_r) \quad . \tag{16}$$

It is not difficult to show that this same relation holds as β_r decreases due to geomagnetic deflection, energy loss and scattering. The factor $1/(1-\beta_r)$ must, of course, be averaged over the angular distribution of the Compton electrons. For 2-MeV gammas, this average is

$$\text{av}\left(\frac{1}{1-\beta_r}\right) \approx 11.2 \tag{17}$$

just after birth of the Compton electrons (Ref. 5). This justifies the factor of 10 used in Section 2.1. In calculations of the HEMP using the continuum Compton current, the expression for this current density is

$$\vec{J}_c = - N_{bp} e\vec{c}\ \text{av}\left(\frac{\vec{\beta}}{1-\beta_r}\right) \quad , \tag{18}$$

where -e is the electron charge. (It is actually the average of $\beta_r/(1-\beta_r)$ that has the value given in equation (17), but β_r is only slightly less than unity.)

2.3 FIELDS RADIATED BY MOVING ELECTRONS

We have seen that the Compton current density averaged over volumes of the order of 1 m^3 has only very small fluctuations in our nominal HEMP problem. This averaged current density is commonly called the macroscopic current density, and is the quantity used in almost all of the applications of electrical engineering, e.g., analysis of radio broadcasting and receiving, electric power generation and transmission, etc. Engineers (and physicists) never try to analyze these problems in terms of

the fields radiated by individual electrons, but have nevertheless been getting correct answers for over 100 years (in fact, since before electrons were discovered). We therefore regard it as curious that quite a few people have insisted that the HEMP must be derived from the radiation of individual electrons in order to obtain reliable results. This seems all the more curious when one recalls that the fields of moving and accelerating electrons are derived in the textbooks by solving Maxwell's (continuum) equations for point charges and currents. Because those equations are linear, it must be true that the average or macroscopic fields are obtained by solving Maxwell's equations with the macroscopic currents.

The reason for the common use of the macroscopic current is that it is generally much easier to add up the currents of a large number of electrons than to add up their fields. However, with sufficient care the latter can be done correctly, as the following simple but relevant examples will show. In this section the essential physics of the examples is described, while the supporting mathematics is worked out in Appendix A.

Example 1. Impulse of Gammas on Thin Sheet

Let us have a planar, impulse function of gammas propagating through vacuum and arriving broadside on a thin insulating sheet, as indicated in figure 3. We imagine that electrons are knocked out of the sheet in the forward direction of the gammas, and that there is a magnetic field B_0 parallel to the sheet, in the y-direction. This field deflects the electrons in semicircles, until they restrike the sheet and are stopped. An observer is located at a distance z_0 below the sheet, which is very large compared with the gyro-radius of the electrons. (This is for ease of calculation.)

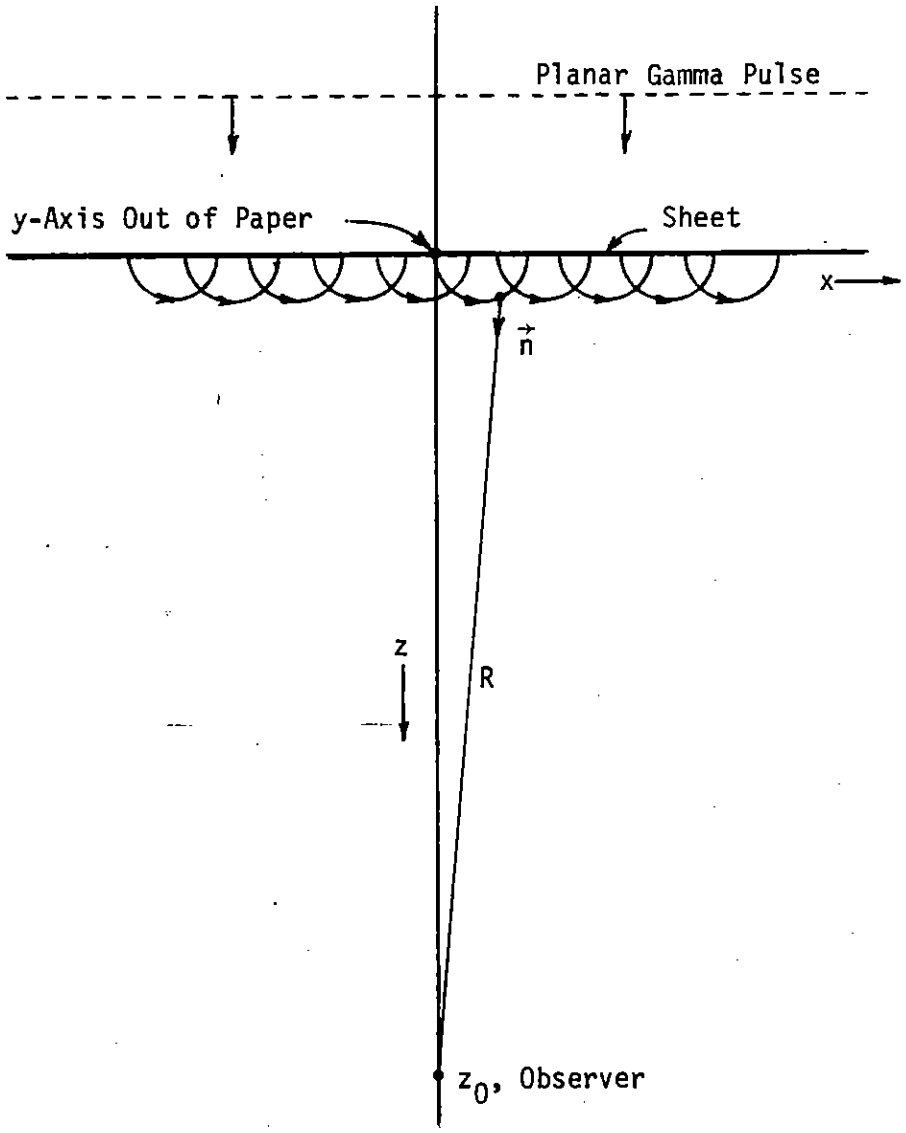

Figure 3. Configuration for Example 1.

We choose the origin of time t such that t = 0 at the instant the gamma pulse arrives at the sheet. The observer, however, elects to trigger his scope on the arrival of the gammas at his location. Thus the time T_0 read on his scope is related to the standard time t by

$$T_0 = t - z_0/c \quad . \tag{19}$$

We shall call T_0 the delayed time at the observer. We can define the delayed time T at any z by

$$T = t - z/c \quad . \tag{20}$$

Thus at any z, T is the time after arrival of the gamma pulse.

Consider now a single electron born at the origin of coordinates. Let the magnitude of its velocity, divided by c, be β and its gyro frequency be ω_e. The latter quantity is (in MKS units)

$$\omega_e = \sqrt{1-\beta^2}\, eB_0/m = \beta c/L \quad . \tag{21}$$

Here m is the rest mass of the electron and L is the gyro radius introduced in Section 2.2. The coordinates and velocity components (again divided by c) are then found to be, as functions of standard time

$$\beta_z = \beta \cos\omega_e t \quad , \quad \beta_x = \beta \sin\omega_e t \quad , \tag{22}$$

$$z_e = L \sin\omega_e t \quad , \quad x_e = L\,(1-\cos\omega_e t) \quad . \tag{23}$$

The distance R from the electron position to the observer is

$$R = \sqrt{(z_0-z_e)^2+x_e^2} \quad . \tag{24}$$

For z_0 large compared with L, R can be expanded in power series in x_e^2 as

$$R = z_0-z_e + \frac{1}{2}\frac{x_e^2}{(z_0-z_e)} + \ldots \tag{25}$$

The transit time of radiated fields from electron to observer is R/c. Dropping the term z_e in equation (25) would make an error in transit time

$$\delta t = -\frac{z_e}{c} \approx \frac{L}{c} \approx \frac{1}{\omega_e} \quad , \tag{26}$$

i.e., comparable with the gyration time and the radiated pulse length. This is too severe an error to accept. Dropping the term in x_e^2 gives an error smaller by the ratio L/z_0, and this is acceptable for large z_0/L. In this case equation (25) is approximated by

$$R = z_0-z_e \quad . \tag{27}$$

Therefore, fields radiated by the electron at standard time t arrive at the observer at standard time

$$t_0 = t + (z_0-z_e)/c \quad . \tag{28}$$

This relation can be written as

$$t_0 - z_0/c = t - z_e/c \quad , \tag{29}$$

or, according to equation (20), as

$$T_0 = T_e \quad . \tag{30}$$

Thus fields are radiated by the electron and arrive at the observer at the same delayed time, in the limit of large z_0/L.

What we have called the delayed time here has been called the retarded time in previous reports on HEMP. However, that is apt to cause confusion with the retarded time as defined in textbooks on electrodynamics. In the present example, the retarded time going with observer time t_0 is the time t in equation (28). In the textbooks, R is not assumed to be large compared with the particle displacement, so that introduction of the delayed time would provide no advantage.

The relation between standard time and delayed time for an electron is generally not simple, depending on the trajectory of the electron. However, the relation between their differentials is simple. From equation (20).

$$\begin{aligned} dT_e &= dt - dz_e/c \\ &= (1-\beta_z)dt \quad . \end{aligned} \tag{31}$$

In the present example, this relation has the integral

$$T_e = t - \frac{L}{c}\sin\omega_e t \quad . \tag{32}$$

For given t, T_e can be found immediately. The inverse relation, i.e., t as a function of T_e, is not expressible in closed form. However, for small $\omega_e t$ we have approximately

$$T_e \approx (1 - \frac{L\omega_e}{c})t = (1-\beta)t \quad . \tag{33}$$

Since for small $\omega_e t$ in our example $\beta \approx \beta_z$, this equation can be written

$$t \approx T_e/(1-\beta_z) \quad , \tag{34}$$

which is the same as equation (31). Either of these equations shows that for an electron moving with β_z close to +1, the delayed time T_e advances small fraction of the rate at which the standard time t advances. Since

$$\omega_e dt = \frac{\omega_e}{1-\beta_z} dT_e \quad , \tag{35}$$

the apparent rate of turning of the electron in the magnetic field in delayed time is much faster than in standard time.

In Appendix A, the electric field radiated by our single electron, born at the origin in figure 3, is calculated. Equations (A-6) and (A-7) express the result. It can be seen that the electric field rises abruptly at t = 0, T_0 = 0 to a peak value

$$E_{xp} = \frac{Z_0}{4\pi} \frac{e\omega_e \beta}{R} \frac{1}{(1-\beta)^2} \quad . \tag{36}$$

The abrupt rise occurs because the electron is immediately accelerated by the magnetic force. E_x then decreases, and changes sign when

$$\cos\omega_e t = \beta \quad , \quad \sin\omega_e t = \sqrt{1-\beta^2} \quad . \tag{37}$$

At this cross-over time, from equation (A-7),

$$\omega_e T_0 = \arcsin(\sqrt{1-\beta^2}) - \beta\sqrt{1-\beta^2} \quad . \tag{38}$$

For 1-MeV electrons, $\beta \approx 0.94$, and the cross-over time becomes

$$\omega_e T_0 = 0.0275 \text{ radians} = 1.58^\circ \quad . \tag{39}$$

Note that at the cross-over time

$$\omega_e t = \arccos(0.94) = 20^\circ \quad . \tag{40}$$

Since in our present example

$$\omega_e = 3.3\times10^6/\text{sec} \quad , \tag{41}$$

the cross-over time is

$$T_0 = 0.83\times10^{-8} \text{ sec} \quad . \tag{42}$$

This result well illustrates how rapidly events occur when viewed as a function of delayed time.

The time-dependent factor in E_x is graphed in figure 4 as a function of T_0, i.e., as it would appear on the observer's scope. Note the very large amplitude at early times. The end of the electron trajectory after one-half turn in the magnetic field corresponds with $\omega_e T_0/\pi = 1$. No more field is radiated to our observer after this time. (The radiation emitted in the starting and stopping of the electron, which may be called bremsstrahlung, vanishes in the z-direction.)

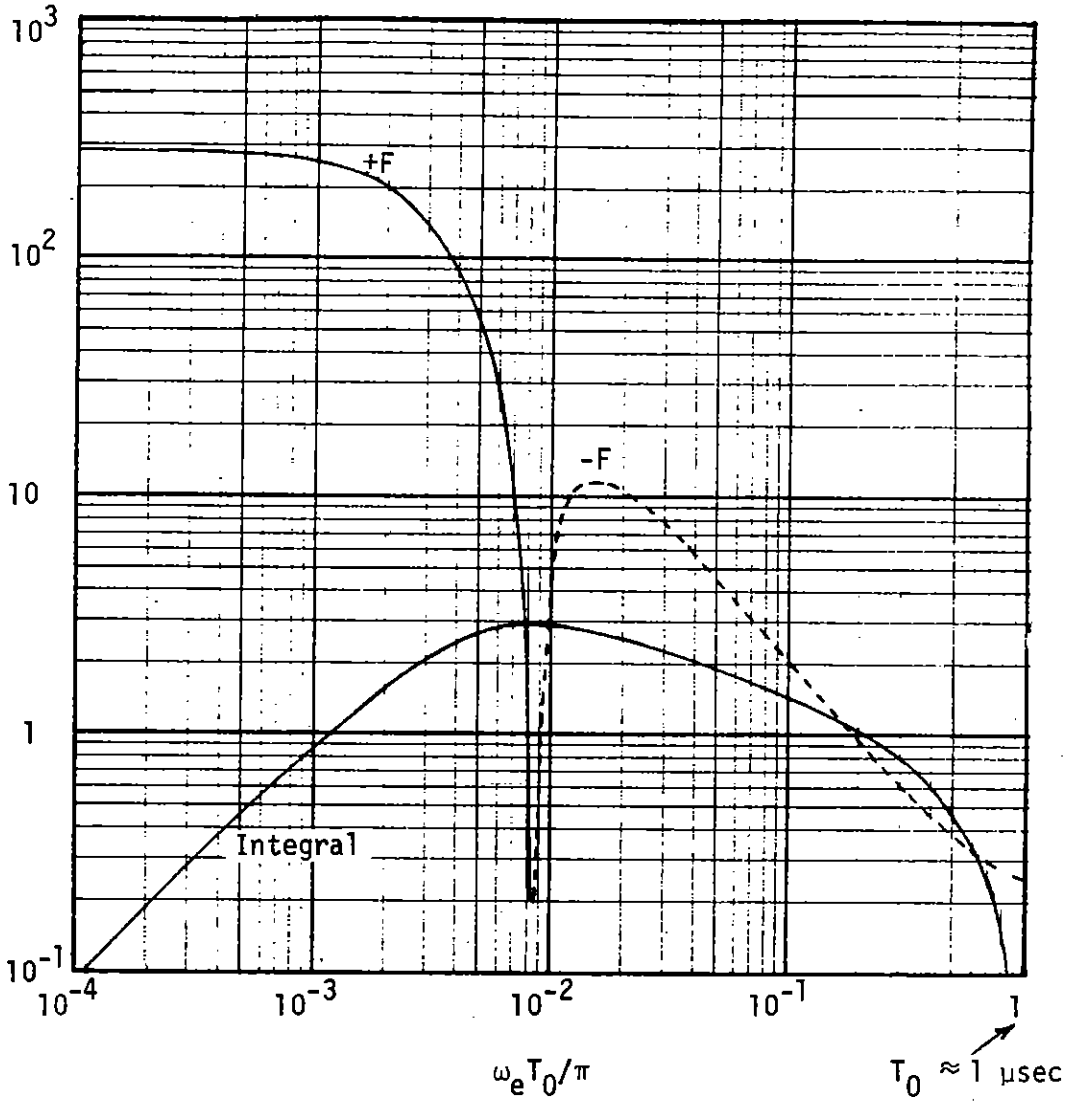

Figure 4. The time-dependent factor $F(T_0) = (\cos\omega_e t - \beta)/(1-\beta\cos\omega_e t)^3$, where $\omega_e T_0 = \omega_e t - \beta\sin\omega_e t$, in the field radiated by an electron with $\beta = 0.94$ that makes one-half turn in a magnetic field. The integral $\int_0^{T_0} F(T)\omega_e dT$ is also shown.

It is also shown in Appendix A that the integral of E_x over T_0 vanishes. The time integral of any radiation field vanishes in the limit as the distance to the observer becomes large compared with the dimension of the radiating system, in this case as z_0/L becomes large.

We can now complete Example 1, by adding up the fields radiated to our observer by electrons born at different positions on the sheet. In doing so there are several points that need to be considered. First, the fields radiated by electrons born away from the origin in figure 3 will be additionally delayed in reaching the observer. Second, the unit vector $\hat{n}$, in the direction from electron to observer, will no longer be in the z-direction, and the vector products in equation (A-1) will change gradually as we move the electron birthplace away from the origin. Third, the direction of the electric field changes when $\hat{n}$ changes.

The most important effect is the additional time delay. The field radiated at standard time t by an electron at z and cylindrical radius ρ from the z-axis reaches the observer at standard time

$$t_0 = t + \sqrt{(z_0-z)^2+\rho^2}/c$$
$$\approx t + (z_0-z)/c + \rho^2/2z_0c \quad . \tag{43}$$

We have again assumed z_0 to be large compared with z and ρ. In terms of the delayed time of observer and electron, this can be written

$$T_0 = T_e + \Delta T \quad , \tag{44}$$

where T_0 and T_e are again defined by equation (20) at the position of observer and electron, and

$$\Delta T \equiv \rho^2/2z_0c \quad . \tag{45}$$

The value of ρ going with a given time delay is then

$$\rho = \sqrt{2z_0 c\Delta T} \quad . \tag{46}$$

Let us see what ρ goes with a time delay equal to the cross-over time for the field radiated by an single electron. For this case, $c\Delta T \approx 3$ m. If we take $z_0 = 3\times10^4$ m, the minimum distance from the HEMP source region to an observer on the ground, we find

$$\rho = 425 \text{ m} \quad . \tag{47}$$

This is only about 5 L, so it might appear that we should have included the x-displacement of the electron in our calculation for the single electron. However, at the cross-over time the x-displacement of that electron was only 0.06 L $\approx$ 5 m (see equation (23)), so that calculation was on safe ground.

For a displacement of 425 m at a distance of 3×10^4, the change in the direction of $\hat{n}$ is only about 0.014 radians $\approx 0.81°$. This is small compared with the 20° deflection of the electron at the cross-over time (equation (40)), so we can neglect the change in the vector products in equation (A-1) to an accuracy of about 4%.

The change in the direction of $\vec{E}$ at the observer is also small. Note that the small z-components of $\vec{E}$ will cancel out when the fields of electrons on opposite sides of the origin are added. The change in E_x is proportional to the change in $\cos(\rho/z_0)$, which is very small.

Thus all we have to do is to sum the field E_x given by equations (A-6) and (A-7) over the electrons at various ρ, with the appropriate time delay, given by equation (45). Let the number of electrons per m^2 of the sheet by N_A. The number of electrons in the differential $d\rho$ is

$$dN_e = 2\pi N_A \rho d\rho = \pi N_A d\rho^2$$

$$= 2\pi z_0 c N_A d(\Delta T) \quad . \tag{48}$$

The net field is then*

$$\overline{E}_x(T_0) = \frac{Z_0}{2} e\beta c N_A \int_0^{T_0} F(T)\omega_e dT \tag{49}$$

where F is the function graphed in figure 4. Note that the factor z_0 in equation (48) has cancelled the factor 1/R in equation (A-6). Thus $\overline{E}_x$ is independent of z_0; it is a plane wave propagating in the z-direction.

The integral in equation (49) is also evaluated in Appendix A. With the result given by equation (A-13), $\overline{E}_x$ becomes

$$\overline{E}_x(T_0) = \frac{Z_0}{2} e\beta c N_A \frac{\sin\omega_e t}{1-\beta\cos\omega_e t} \quad , \tag{50}$$

where the relation of T_0 to t is again given by equation (A-7).

We see that $\overline{E}_x(T_0)$ is positive for $\omega_e t < \pi$ (which according to equation (A-6) is the same condition as $\omega_e T_0 < \pi$), but vanishes at $\omega_e T_0 = \pi$.

---

* Note that $\int_0^{T_0} F(T_0-\Delta T)d\Delta T = \int_0^{T_0} F(T)dT$.

Thus the integral of $\overline{E}_x$ over T_0 does not vanish. While $\overline{E}_x$ is a radiated wave, we have taken the sheet to have unlimited dimension. At times after signals can arrive at the observer from the actual edge of the sheet, there will be additional $\overline{E}_x$, and the total time integral of $\overline{E}_x$ will vanish. This must be so, since the time integral for each single electron vanishes.

The time dependent factor in equation (50) is also graphed in figure 4. It rises linearly with T_0 at early T_0, has a maximum at the cross-over time of the single-electron field, and goes linearly to zero at $T_0 = \pi/\omega_e$. The maximum value of this factor is

$$I_{max} = 1/\sqrt{1-\beta^2} = 2.93 \text{ for } \beta = 0.94 \quad . \tag{51}$$

Persons familiar with the outgoing wave theory will already see that equation (50) is in exact agreement with the result that can be derived very simply from that theory. Before we demonstrate this fact, it is useful to consider two additional examples.

Example 2. Steady Flux of Gammas

Let us now have a steady flux of gammas on the thin sheet. Each individual electron will radiate field as in Example 1. Now adding up the fields radiated by the electrons in a small volume near the origin, we have to add the fields due to electrons born at different times (before we consider different ρ's). This addition amounts to integrating the field E_x of a single electron over T_0, and we have seen that this integral vanishes. Thus there is no radiated macroscopic field in this case.

The reason is that, while there is a macroscopic current density in this case (in the x-direction), the time derivative of this current density vanishes. In order to have a radiated macroscopic field, there must exist a macroscopic current density with non-vanishing time derivative.

Note that if we first add up the fields of electrons born at the same time but at different ρ, we get the $\overline{E}_x$ of Example 1. If we then add up the $\overline{E}_x$ for electrons born at different times, we do not get zero because $\overline{E}_x$ is never negative. As a lesson in the care that must be taken in adding the fields of individual electrons, we leave it to the reader to explain this paradox.

Example 3. Impulse of Gammas on Several Sheets

Let us now have several parallel sheets close to each other, but imagine that a sheet has no effect on the electrons born in other sheets. Let the same impulse of gammas traverse the region containing the sheets.

It is clear that the signals from all of the sheets will arrive at the observer at the same time, since both the gammas and the signal travel at the speed c. The observer cannot tell whether there is one sheet or several. He can only deduce, by comparing his experimental data with equation (50), the total areal density N_A of electrons summed over all sheets.

This example can be extended directly to a continuous medium, provided we keep the same electron trajectories. Then N_A in equation (50) is replaced by

$$N_A = N_{bp}\Delta z \tag{52}$$

for uniform electron birthplace density N_{bp} over a region of thickness Δz, or by

$$N_A = \int N_{bp}\, dz \tag{53}$$

if N_{bp} is variable, e.g., due to gamma attenuation.

In Section 2.4 we derive these same results from the outgoing wave theory in an almost trivial way. Before taking up that task, let us look again at the number of electrons that contribute (coherently) to the signal seen by the observer. This number depends on the delayed time. According to equation (46), the number of electrons that contribute at delayed time T is

$$N_{con} = \pi\rho^2 N_A = 2\pi z_0 cT N_A \quad . \tag{54}$$

Choosing $T = 10^{-9}$ sec, $z_0 = 3\times10^4$ m, and choosing N_A at this time to be $1/10$ of the value given by equation (9) gives

$$N_{con} = 3.6\times10^{18} \text{ electrons.} \quad (0.58 \text{ Coulombs}) \tag{55}$$

The fractional fluctuation in this number is less than 1 in 10^9. Thus adding the fields by doing integrals rather than by a discrete sum, as we have done, is clearly justified to very high accuracy.

2.4 THE OUTGOING WAVE EQUATION

It has been alleged on more than one occasion that our theory of HEMP does not conserve energy. In this section we derive the outgoing wave equation directly from the conservation of energy. This is done first in planar geometry; the equation is then applied to Example 3 of Section 2.3, with results identical to equations (50) and (53). The outgoing wave equation is then derived in spherical geometry and the diffraction problem is defined and discussed in simple but approximate terms.

Planar Geometry

Consider a plane electromagnetic wave propagating in the z-direction, with the electric field in the x-direction. For such a wave,

$$E_x = E_x\left(t - \frac{z}{c}\right) \quad , \tag{56}$$

i.e., E_x depends on the difference of t and z/c, not on t and z separately. This combination of t and z is what we have called the delayed time in Section 2.3,

$$T = t - \frac{z}{c} \quad , \tag{57}$$

which, for any z, is the time after the arrival of the gamma pulse. Thus the field

$$E_x = E_x(T) \tag{58}$$

is the field an observer at z would see on his scope if he triggered the horizontal sweep on the arrival of the gamma pulse. In this case, the amplitude and shape of the electromagnetic wave is the same for all (stationary) observers, independent of their z. Such propagation is appropriate in vacuum where there are no sources or absorbers of energy.

If we have plane-symmetric sources and absorbers of energy, then observers at different z may observe different E_x, i.e.,

$$E_x = E_x(T,z) \quad . \tag{59}$$

The symbol $E_x(T,z)$ means the field an observer at z would see on his gamma-triggered scope.

The power flow density in the wave is

$$P(T,z) = E_x^2(T,z)/Z_0 \text{ watts/m}^2 \quad , \tag{60}$$

where

$$Z_0 \approx 120\pi \approx 377 \text{ ohms} \quad . \tag{61}$$

With sources and absorbers present, observers at different z may see different power densities at the same T. Energy is put into or taken from electromagnetic fields by currents flowing against or in the direction of the electric field. If $J_x(T,z)$ is the current density in Amps/m^2, then

$$J_x E_x \text{ watts/m}^3 \tag{62}$$

is the power/m^3 being taken out of the fields and put into the current (electrons). This energy transfer to the electrons must decrease the power flow density in the wave. Considering two z's a differential dz apart, we can write the law of energy conservation as

$$\frac{\partial}{\partial z} \frac{E_x^2}{Z_0} \left(\frac{\text{watts}}{m^3}\right) = - J_x E_x \left(\frac{\text{watts}}{m^3}\right) \quad . \tag{63}$$

The partial derivative here means that T is held constant; energy taken out of the wave near time T reduces the power flow density near that time, and the notch in the wave so produced propagates along with the wave. Now carrying out the differentiation of E_x^2 gives

$$\frac{\partial}{\partial z} E_x = - \frac{Z_0}{2} J_x \quad . \tag{64}$$

Here J_x is the total current density. If we have both Compton current J_{xc} and conduction current σE_x, with σ the conductivity, then

$$\frac{\partial}{\partial z} E_x = - \frac{Z_0}{2} (J_{xc}+\sigma E_x) \quad . \tag{65}$$

This is the outgoing wave equation in planar geometry, first derived in Reference 1. It is called outgoing because the wave propagates in the same direction as the gammas. The Compton current, driven by the gammas, appears therefore to move with the gammas, so that the variables T,z are also convenient for expressing $J_{xc}(T,z)$.

Application to Example 3

In Example 3 we neglected any conductivity. Putting $\sigma = 0$ in equation (65) and integrating z through the source region gives

$$E_x(T) = - \frac{Z_0}{2} \int J_{xc}(T,z)dz \quad . \tag{66}$$

The macroscopic Compton current density is

$$J_{xc} = - ev_x N_{ce} \quad , \tag{67}$$

where $v_x = \beta_x c$ is the electron velocity component and N_{ce} is the density of Compton electrons, which is related to the density N_{bp} of Compton electron birthplaces by equation (16). Thus

$$E_x(T) = \frac{Z_0}{2} ec \int \frac{N_{bp}(z)\ \beta_x(T)}{1-\beta_z(T)} dz \quad . \tag{68}$$

For Example 3, β_x and β_z are given by equation (22), i.e.,

$$\beta_z = \beta\cos\omega_e t \quad , \quad \beta_x = \beta\sin\omega_e t \quad , \tag{69}$$

where t is related to T by (equation (A-7))

$$\omega_e T = \omega_e t - \beta\sin\omega_e t \quad . \tag{70}$$

Therefore the final expression for E_x is

$$E_x(T) = \frac{Z_0}{2} e\beta c \left(\int n_{bp} dz\right) \frac{\sin\omega_e t}{1-\beta\cos\omega_e t} \quad . \tag{71}$$

This is identical with equation (50), with equation (53) for N_A. Recall that N_A is also equal to the number of gammas per m^2 incident on the atmosphere.

Probably most readers will agree that the calculation of E_x here is simpler and more reliable than that in Section 2.3 based on adding the fields radiated by individual electrons.

The peak value of E_x occurs at $\cos\omega_e t = \beta$ and is

$$E_{xp} = \frac{Z_0}{2} \frac{e\beta c}{\sqrt{1-\beta^2}} N_A \quad . \tag{72}$$

With $\beta = 0.94$ (1-MeV electrons) and $N_A = 6.5\times10^{-14}/m^3$ (equation (9)), this becomes

$$E_{xp} = 1.6\times10^7 \text{ V/m} \quad . \tag{73}$$

The HEMP is actually never this large, the chief reason being the severe attenuation due to air conductivity. While the effect of air conductivity is easily calculated from the outgoing wave equation, it is very difficult to include accurately in the individual electron calculation.

Spherical Geometry

The derivation of the outgoing wave equation given above for planar geometry is easily modified for spherical geometry. In this case the gammas come from a source with dimensions of the order of a meter in a time span of the order of 10^{-8} second. Thus at later times the gammas occupy a spherical shell, centered about the burst point, and with thickness of a few meters. The Compton current is produced in the part of this shell that intersects the atmosphere at altitudes below 50 km or so. It is clear that outgoing spherical waves will be generated if the Compton current has components transverse to the radius vector from the burst point, and the geomagnetic field ensures that there will be such currents. The wavelengths in these waves will be of the order a few meters to tens of meters (to fit into the shell). Because of the large radius of the shell, from burst point to source region, variation of the wave with transverse distances will be very slow compared with variation with radial distance. This means that the waves propagate approximately in the radial direction, since they propagate in the direction of their gradients.

If observers trigger their scopes on arrival of the gamma pulse, then the delayed time T for them in the spherical case is related to standard time t by

$$T = t - \frac{r}{c} \quad , \tag{74}$$

where r is the distance from the burst point. The transverse wave electric field E_t will now be a function of T and r. In a fixed element $\delta\Omega$ of solid angle, the power flow is

$$P(T,r) = \frac{E_t^2(T,r)}{Z_0} r^2 \delta\Omega \text{ watts} \quad . \tag{75}$$

If there is a current J_t in the direction of E_t, then the power flow will vary with r according to

$$\frac{\partial}{\partial r}\left(\frac{E_t^2(T,r)}{Z_0} r^2 \delta\Omega\right) = - J_t(T,r) \underset{\hat{r}}{E_t} r^2 \delta\Omega \frac{\text{watts}}{\text{m}} \quad ,$$

or

$$\frac{1}{Z_0}\frac{\partial}{\partial r}(rE_t)^2 = r^2 J_t E_t \quad . \tag{76}$$

Carrying out the derivative leads to

$$\frac{\partial}{\partial r}(rE_t) = - \frac{Z_0}{2} rJ_t$$

$$= - \frac{Z_0}{2} r(J_{tc}+\sigma E_t) \quad . \tag{77}$$

Here we have expressed the total transverse current as the sum of Compton and conduction parts. This is the outgoing wave equation in spherical geometry, and was first derived by Karzas and Latter in Reference 2.

Comparison of equations (65) and (77) shows that the only difference is the replacement of E_t by rE_t in the spherical case and J_t by rJ_t. This replacement coincides with the fact that, in a case without Compton current and conductivity, E_t is independent of z in the planar case while rE_t is independent of r in the spherical case.

If the burst point is very far away from the source region, then the factor r varies little in the source region. In this case, the planar equation (65) can be used in the source region, but we should remember that the amplititude of the HEMP will fall, after it is produced, inversely proportional to the distance from the burst point.

Equations (65) and (77) replace the full set of 6 Maxwell equations with partial derivatives in 3 space coordinates and time. They make it possible to understand the HEMP in quite simple terms, and to find approximate analytical solutions. They also make it possible to find numerical solutions, that are accurate to a few percent, with modest rather than prohibitive amounts of computer time.

Effect of Conductivity; Saturation

It is easy to understand the effect of conductivity from either of equations (65) or (77). In the planar case, if there is no Compton current, $J_{xc} = 0$, then E_x attenuates with distance according to

$$E_x(T,z) = E_{xo}(T) \exp\left[-\frac{Z_0}{2}\sigma z\right] \quad . \tag{78}$$

The attenuation length is $2/Z_0\sigma$, which becomes shorter for larger σ. Thus two effects oppose each other in equation (65). As the wave moves along in z, its amplitude is increased by the Compton current in the direction of $-J_{xc}$. The minus sign here is an example of Lenz's law. At the same time, the wave is attenuated by the conductivity. These two opposing effects balance if the right-hand side of equation (65) vanishes, i.e., $\partial E_x/\partial z = 0$ if

$$E_x = - J_{xc}/\sigma \quad . \tag{79}$$

This field, for which the Compton current is cancelled by the conduction current, is called the saturated field. The HEMP field approaches this value in the source region when the attenuation length becomes small compared with the thickness of the source region. Note that the saturated field is the same in planar and spherical geometry.

Below the source region, where the gammas have been mostly scattered, both J_{xc} and σ become small, but the saturated field changes only a little. When J_{xc} and σ become sufficiently small, the HEMP propagates as a free wave without further buildup or attenuation. The 1/r dependence is still present, of course.

The solution of the outgoing wave equation is discussed in detail in References 5 and 6.

Diffraction

In our derivation of the outgoing wave equations, we assumed that energy flow was strictly in the z- or r- directions in the planar or spherical cases, respectively. In the real, spherical case, this was justified by the argument that the transverse variations of the wave are small compared with the radial variations. The wave must have transverse variations since there are no spherical waves that are independent of the angles of spherical coordinates. The wave must be composed of spherical harmonics Y_ℓ^m (in the standard notation) with $\ell \geq 1$. Generally, however, the minimum length scale of the transverse variations is set by the

atmospheric scale height, equation (8), since the gamma flux and Compton current will vary significantly in this distance. For observers that are near the horizon from a given burst point, as sketched in figure 5, the vertical direction is not far from the θ-direction of spherical coordinates. In this case, the scale length of wave variations in θ is indeed approximately the scale height h. The scale length for variations in the azimuthal direction ϕ is comparable with the radius of the source region from the burst point, which is typically much greater than h; this variation comes from the changing angle between the newborn Compton electrons and the geomagnetic field. Thus the principal transverse variations are those associated with the scale height.

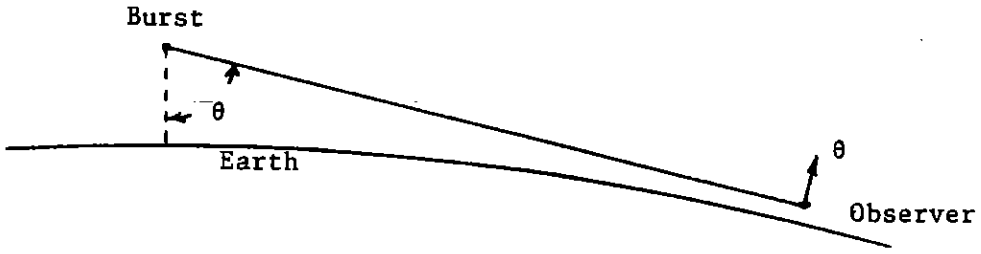

Figure 5. For an observer near the horizon, the θ-direction is approximately vertical.

The effect of these variations is to produce diffraction of the wave as it propagates on outward from the source region. The theory of diffraction of spherical EM waves is developed in detail in Section 3. At present we use an approximate argument to show why the effect of diffraction expected to be small.

Let us take the wavelength in the EMP to be

$$\lambda \approx 30 \text{ m} \quad . \tag{80}$$

Let us imagine that the HEMP as seen by an observer near the horizon is produced entirely in a slit of width h. This would seem to over-estimate the diffraction, since it takes no benefit from the free spherical wave existing below the source region (see figure 5), which should join on to the lower edge of the new wave generated in the slit. Now the distance of travel of a (planar) beam of width h before the diffraction effects reach its center is

$$s \approx h^2/\lambda \approx 1500 \text{ km} \quad . \tag{81}$$

This distance is substantially larger than the distance ≈ 600 km from an observer on the horizon to the source region on his ray from the burst point. Even so, this planar diffraction estimate suggests that diffraction effects could amount to several percent for the horizon observer. Actually, we shall find that spherical diffraction is substantially less than planar diffraction. An outgoing spherical wave, once it is well into the wave zone for all of its spherical harmonic components, does not undergo further change in its angular dependence.

2.5 BREMSSTRAHLUNG

The EMP that we have calculated thus far in this report is due to the deflection of the Compton electrons by the geomagnetic field. There are additional mechanisms by which Compton electrons radiate. Two of these are described here.

The Compton scattering process produces a moving electron suddenly. Both classically and quantum mechanically, a sudden change in the velocity of a charged particle leads to the emission of radiation. This is in addition to the scattered gamma in the original Compton scattering process. In quantum mechanics, there can be two, or more, photons in the final state, and the sum of the energies of these photons can approach the energy of the initial photon. We need to distinguish between the additional photons that have energies that are an appreciable fraction of that of the initial photon and those that have very small energies.

The probability that there will be an additional photon of substantial energy in the final state is of the order of $e^2/\hbar c \approx 0.01$. Thus this is a fairly rare occurrence. Furthermore, the additional photon will be subsequently scattered by the air like any other gamma, and the existence of the additional photon will cause no significant change in the EMP produced.

The probability that there will be additional photons of very low energy is large. In fact, the total number of low energy photons is (in lowest order) logarithmically infinite, since the number of photons per unit photon energy E_p is proportional to

$$N(E_p)\, dE_p \sim dE_p/E_p \sim d\omega/\omega \quad . \tag{82}$$

Here we have used the Planck relation $E_p = \hbar\omega$, where ω is the photon angular frequency and $\hbar$ is the reduced Planck constant. Further, the emission of the low-frequency radiation can be computed classically.

The question now arises whether this low-frequency radiation will add coherently from the multitudinous Compton scattering events, as the geomagnetic EMP does. Since the birthplaces and birth times of Compton electrons are random, except that radial position and time are correlated to within the gamma pulse duration by the speed c of the initial gammas, the only possible direction in which the phases of the various emissions can add constructively is the forward or radial direction. In this direction, the question is how many electrons can contribute signals that are approximately in phase to a given observer. This question was answered for the geomagnetic EMP at the end of Section 2.3, equation (55). For frequencies less than $\omega = 10^9$/sec, for which the time delay for phase coherence is 10^{-9} sec or less, the number of electrons is of the order of 10^{18}. Now the fraction of the Compton electron energy E_{ce} radiated at frequencies less than $\omega = 10^9$ is

$$f(\omega) \approx 0.01\ \hbar\omega/E_{ce} \approx 10^{-20}\ \text{ergs}/E_{ce}$$

$$\approx 10^{-14} \text{ for } E_{ce} \approx 1 \text{ MeV} \quad . \tag{83}$$

This is for a single radiating electron. Taking into account the addition of fields from 10^{18} electrons, the energy radiated per electron has to be multiplied by a number that is of the order of magnitude 10^{18}. Since this would make the fractional energy radiated per electron larger than unity, it is clear that reaction of the radiated fields on the electrons would limit the actual radiated fraction, presumably to a value not far from unity. Thus the radiation from the starting of the Compton electrons would be a large effect, at least comparable to the geomagnetic EMP, were it not for the fact that the sum of these radiated fields of individual electrons is actually zero except for fluctuation effects. The reason is explained in figure 6. Opposite fields are radiated in the forward direction by two Compton electrons whose transverse velocity components are opposite. Since the Compton electron angular distribution is symmetrical with respect to reversal of the transverse velocity, the radiated fields for a given transverse velocity and its opposite cancel exactly in

the forward direction. Only fluctuations in the actual Compton electron distribution will radiate. For these the radiated fields of an individual electron to be multiplied by $\sqrt{10^{18}} = 10^{9}$, and the radiated noise energy per electron is $10^{9} \times 10^{-14} = 10^{-5}$ of the Compton electron energy. These numbers are rough order-of-magnitude only, and will depend on the frequencies considered. The noise is focussed in the forward direction, but is attenuated at later times by air conductivity.

The effect described above could be called a type of bremsstrahlung. The Compton electrons also emit true bremsstrahlung in their collisions with the nuclei of air atoms. Because the Compton electrons do not move radially with the speed of light, the noise so radiated should be essentially incoherent, roughly isotropic in direction with power equal to the sum of the powers radiated by individual electrons.

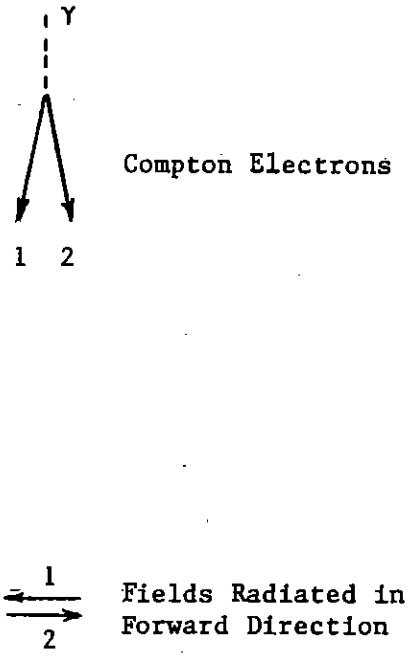

Figure 6. Cancellation in forward direction of fields radiated due to sudden start of Compton electrons.

SECTION 3
SPHERICAL DIFFRACTION

The goal of this section is to find a way to extrapolate outgoing spherical waves from a radius r_1 to larger r, including $r = \infty$. The radius r_1 is the outer radius of the source region, so that the Compton current and the air conductivity may be assumed to vanish in the region of interest. In this region Maxwell's equations take the form

$$\frac{1}{c}\frac{\partial \vec{B}}{\partial t} = -\nabla \times \vec{E} \quad , \tag{84}$$

$$\frac{1}{c}\frac{\partial \vec{E}}{\partial t} = \nabla \times \vec{B} \quad . \tag{85}$$

Note that these equations are invariant to the replacement $\vec{E} \to \vec{B}$, $\vec{B} \to -\vec{E}$; the two equations are simply interchanged by this replacement. Therefore, any relation between $\vec{E}$ and $\vec{B}$ derived from the equations will also be valid under the replacement. We shall call equations related by the replacement <u>images</u> of each other. Thus equations (84) and (85) are images of each other.

Taking the dot product of $\vec{r}$ with equation (84) yields

$$\frac{1}{c}\frac{\partial}{\partial t}(\vec{r} \cdot \vec{B}) = -\vec{r} \cdot \nabla \times \vec{E} = -(\vec{r} \times \nabla) \cdot \vec{E} = -\vec{L} \cdot \vec{E} \quad , \tag{86}$$

where,

$$\vec{L} = \vec{r} \times \nabla \quad . \tag{87}$$

This operator is the angular momentum operator of quantum mechanics, apart from a constant factor. Of more immediate relevance, it involves derivatives only in directions transverse to $\vec{r}$; i.e., only with respect to the angular coordinates θ and ϕ of spherical coordinates.

Equation (86) can be written

$$\frac{1}{c}\frac{\partial}{\partial t}(rB_r) = -\vec{L} \cdot \vec{E} \quad . \tag{88}$$

The image of this equation is

$$\frac{1}{c}\frac{\partial}{\partial t}(rE_r) = \vec{L} \cdot \vec{B} \quad . \tag{89}$$

We can also find alternative expressions for these two time derivatives. Since $\nabla \times \vec{r} = 0$, proceeding from the second step in equation (86) yields

$$\frac{1}{c}\frac{\partial}{\partial t}(rB_r) = -(\vec{r} \times \nabla) \cdot \vec{E} = \nabla \times \vec{r} \cdot \vec{E} = \nabla \cdot (\vec{r} \times \vec{E}) \quad . \tag{90}$$

The image of this equation is

$$\frac{1}{c}\frac{\partial}{\partial t}(rE_r) = -\nabla \cdot (\vec{r} \times \vec{B}) \quad . \tag{91}$$

The appearance of the cross products in these equations suggests that we should cross $\vec{r}$ with equations (84) and (85). The first of these yields

$$\frac{1}{c}\frac{\partial}{\partial t}(\vec{r}\times\vec{B}) = -\vec{r}\times(\nabla\times\vec{E}) = (\vec{r}\cdot\nabla)\vec{E} - \nabla_{(E)}(\vec{r}\cdot\vec{E}) \quad .$$

where, in the last term, $\nabla_{(E)}$ operates only on $\vec{E}$. We can rewrite this as

$$\frac{1}{c}\frac{\partial}{\partial t}(\vec{r}\times\vec{B}) = (\vec{r}\cdot\nabla)\vec{E} - \nabla(\vec{r}\cdot\vec{E}) + \nabla_{(r)}(\vec{r}\cdot\vec{E}) \quad ,$$

where $\nabla_{(r)}$ operates only on $\vec{r}$. Working out this term in Cartesian components r_i and E_i gives

$$\nabla_{(r)}(\vec{r}\cdot\vec{E}) = \sum_i E_i\nabla r_i = \vec{E} \quad .$$

Therefore

$$\frac{1}{c}\frac{\partial}{\partial t}(\vec{r}\times\vec{B}) = (r\frac{\partial}{\partial r})\vec{E} + \vec{E} - \nabla(rE_r) \quad .$$

$$= \frac{\partial}{\partial r}(r\vec{E}) - \nabla(rE_r) \quad . \qquad (92)$$

The left hand side of this equation has no radial component. It can be seen that the right hand side doesn't either. To show this one needs to use the fact that the radial derivatives of the unit vectors $\vec{r}_0$, $\vec{\theta}_0$ and $\vec{\phi}_0$, which enter into $\vec{E}$, all vanish. (Their derivatives with respect to θ and ϕ do not vanish.)

Equations (88), (89), (92) and the image of (92) are equivalent to the Maxwell equations (84) and (85). We have separated the fields into radial and transverse parts.

3.1 THE RADIAL FIELDS

Taking the time derivative of equation (91) and using equation (92) gives

$$\frac{1}{c^2}\frac{\partial^2}{\partial t^2}(rE_r) = -\nabla \cdot [(\vec{r} \cdot \nabla)\,\vec{E} + \vec{E} - \nabla(rE_r)] \quad . \tag{93}$$

Now $\nabla \cdot \vec{E} = 0$ since there are no charge densities in the region of interest. (Note that taking the divergence of equation (85) gives $\partial(\nabla \cdot \vec{E})/\partial t = 0$; thus if $\nabla \cdot \vec{E} = 0$ initially, it will remain so.) Further, using Cartesian coordinates gives

$$\nabla \cdot (\vec{r} \cdot \nabla)\,\vec{E} = \sum_{i,j} \frac{\partial}{\partial r_i}\, r_j \frac{\partial}{\partial r_j} E_i$$

$$= \sum_{i,j} \left(\delta_{ij} \frac{\partial}{\partial r_j} E_i + r_j \frac{\partial}{\partial r_j}\frac{\partial}{\partial r_i} E_i\right)$$

$$= \nabla \cdot \vec{E} + (\vec{r} \cdot \nabla)\,\nabla \cdot \vec{E} = 0 \quad .$$

Therefore equation (93) becomes

$$\frac{1}{c^2}\frac{\partial^2}{\partial t^2}(rE_r) = \nabla^2(rE_r) \quad . \tag{94}$$

The image of this equation is

$$\frac{1}{c^2}\frac{\partial^2}{\partial t^2}(rB_r) = \nabla^2(rB_r) \quad . \tag{95}$$

Thus we see that the scalars $\vec{r} \cdot \vec{E}$ and $\vec{r} \cdot \vec{B}$ must satisfy the scalar wave equation.

The general solution of the scalar wave equation in spherical coordinates r, θ, ϕ is found by making use of the well-known decomposition of ∇^2 into radial and angular derivatives. For any scalar function ψ,

$$\nabla^2\psi = \frac{1}{r^2}\frac{\partial}{\partial r} r^2 \frac{\partial \psi}{\partial r} + \frac{1}{r^2} L^2\psi \quad . \tag{96}$$

(This decomposition is verified by writing $L^2\psi = (\vec{r} \times \nabla) \cdot (\vec{r} \times \nabla\psi) = \vec{r} \cdot (\nabla \times (\vec{r} \times \nabla\psi))$ and working out the triple cross product.). The eigenfunctions of the operator L^2 are the spherical harmonics $Y_{\ell m}(\theta, \phi)$, and

$$L^2 Y_{\ell m} = -\ell(\ell + 1)\, Y_{\ell m} \quad . \tag{97}$$

One solution of equation (94) is then

$$rE_r = \frac{1}{r} R(r,t)\, Y_{\ell m}(\theta, \phi) \tag{98}$$

where the function R (r,t) is found by substituting this expression into equation (94). The result is

$$\frac{1}{c^2}\frac{\partial^2 R}{\partial t^2} = \frac{\partial^2 R}{\partial r^2} - \frac{\ell(\ell + 1)}{r^2} \quad . \tag{99}$$

Usually this radial equation is solved by going to the Fourier domain, but it is more convenient to stay in the time domain. We look for an <u>outgoing wave</u> solution by trying R of the form

$$R(r,t) = f_0(T) + \frac{1}{r} f_1(T) + \frac{1}{r^2} f_2(T) + \ldots \tag{100}$$

where T is the delayed time

$$T = t - \frac{r}{c} \quad . \tag{101}$$

For R a function of r and T, equation (99) becomes

$$\left(\frac{2}{c}\frac{\partial}{\partial T} - \frac{\partial}{\partial r}\right)\frac{\partial R}{\partial r} = -\frac{\ell(\ell+1)}{r^2} R \quad . \tag{102}$$

When the expression in equation (100) is substituted in this equation and the coefficients of the power $1/r^{n+1}$ collected on both sides and set equal, the result is a relation between f_{n-1} and f_n,

$$\frac{2}{c} n \frac{df_n}{dT} = [\ell(\ell+1) - (n-1)n]f_{n-1} \quad . \tag{103}$$

Putting $n = 0$ gives $f_{-1} = 0$, whereas $n = 1$ yields

$$\frac{2}{c}\frac{df_1}{dT} = \ell(\ell+1)\, f_0 \quad . \tag{104}$$

Thus the series starts correctly with f_0, and f_0 (T) is completely arbitrary. The function f_1 is proportional to the T-integral of f_0, f_2 is proportional to the T-integral of f_1, and so on. Since the right hand side of equation (103) vanishes for $n = \ell + 1$, the series terminates after $n = \ell$. (Since $E_r \sim R/r^2$, the powers in E_r range from $1/r^2$ to $1/r^{\ell+2}$.) Equation (100) therefore does provide a well-behaved solution of outgoing-wave type. Changing the minus sign in equation (101) to a plus sign would yield an ingoing-wave solution.

The general solution for rE_r is a sum of terms of the type of equation (98) with all possible ℓ and m, where each $Y_{\ell m}(\theta,\phi)$ has its own factor $R_{\ell m}(r,t)$. This general solution can obviously be written as a power series in $1/r$ by collecting coefficients of the same power together,

$$r^2E_r = F_0(T, \theta, \phi) + \frac{1}{r} F_1(T, \theta, \phi) + \frac{1}{r^2} F_2 + \ldots \qquad (105)$$

The recursion relation between F_n and F_{n-1} is

$$\frac{2}{c} n \frac{dF_n}{dT} = - [L^2 + (n-1)\, n]\, F_{n-1} \qquad (106)$$

Once again, F_0 is completely arbitrary, both as to its T-dependence and its dependence on θ and ϕ. F_1, F_2, etc., are then determined as time integrals of F_n with lower n, operated on by the operator on the right-hand side of equation (106).

If $r^2E_r(T, r, \theta, \phi)$ is known at some value $r = r_1$, the expansion (105) and the recursion relations (106) allow determination of all of the F_n. From these, r^2E_r is determined for all other r outside the source region (i.e. where Compton current and conductivity vanish). Thus given E_r at an r just outside the source region, E_r can be calculated at all larger r. The same is true, of course, for B_r. We could use these facts to extrapolate the EMP to larger distances, but we need to evaluate also the transverse fields. These fall off only as $1/r$, whereas E_r and B_r fall off as $1/r^2$, in the limit of large r.

3.2 THE TRANSVERSE FIELDS

We pointed out just after equation (92) that that equation had no radial component on either side. No information will be lost, therefore, in crossing the unit vector $\vec{r}_0$ with it. Note that

$$\frac{\partial}{\partial t}\vec{r}_0 = 0 = \frac{\partial}{\partial r}\vec{r}_0 \quad , \tag{107}$$

and

$$\vec{r}_0 \times (\vec{r} \times \vec{B}) = \vec{r}\,(\vec{r}_0 \cdot \vec{B}) - (\vec{r}_0 \cdot \vec{r})\,\vec{B}$$

$$= -r\vec{B} + \vec{r}\,B_r = -r\vec{B}_t \quad , \tag{108}$$

where $\vec{B}_t$ is the part of $\vec{B}$ transverse to $\vec{r}$. The result of the crossing is therefore

$$\frac{1}{c}\frac{\partial}{\partial t} r\vec{B}_t = -\frac{\partial}{\partial r}(\vec{r} \times \vec{E}_t) + \frac{1}{r}\vec{L}\,(rE_r) \tag{109}$$

The image of this equation is

$$\frac{1}{c}\frac{\partial}{\partial t} r\vec{E}_t = \frac{\partial}{\partial r}(\vec{r} \times \vec{B}_t) - \frac{1}{r}\vec{L}\,(rB_r) \tag{110}$$

These equations relate the transverse parts of $\vec{B}$ and $\vec{E}$ to each other and to E_r and B_r. Together with equations (88) and (89) they are completely equivalent to the Maxwell equations (84) and (85).

Let us examine the angular dependence of $\vec{B}_t$ and $\vec{E}_t$. Assume first that the scalar $\vec{r} \cdot \vec{E} = rE_r \equiv \psi$ is nonvanishing, and let it have

the angular dependence of some particular $Y_{\ell m}$. Equation (109) then indicates that a possible consistent angular dependence of $\vec{B}_t$ and $\vec{r} \times \vec{E}_t$ is

$$\vec{B}_t \sim \vec{L}\psi \sim \vec{r} \times \vec{E}_t \quad . \tag{111}$$

The second proportionality here leads to

$$\vec{r} \times (\vec{r} \times \vec{E}_t) \sim \vec{r} \times \vec{L}\psi$$

or

$$- r^2 \vec{E}_t \sim \vec{r} \times (\vec{r} \times \nabla\psi) = - r^2 \nabla_t \psi \quad ,$$

where ∇_t is the transverse part of the gradient operator. Thus our first assumption (non-vanishing E_r) leads to the angular dependences

$$\vec{B}_t \sim \vec{L}\psi \quad , \quad \vec{E}_t \sim \nabla_t \psi \quad . \tag{112}$$

Let us see if these results are consistent with equations (88) and (89). Note that

$$\vec{L} \cdot \vec{E} = (\vec{r} \times \nabla) \cdot \vec{E} = \vec{r} \cdot \nabla \times \vec{E} = r(\nabla \times \vec{E})_r \quad . \tag{113}$$

The last form shows that only the transverse components of $\vec{E}$ are involved in $\vec{L} \cdot \vec{E}$. Therefore

$$\vec{L} \cdot \vec{E} = r(\nabla \times \nabla_t \psi)_r = r(\nabla \times \nabla\psi)_r = 0 \quad , \tag{114}$$

since the curl of the gradient of a scalar function vanishes identically. Equation (88) then indicates that

$$B_r = 0 \quad . \quad \text{(in first case)} \tag{115}$$

Equation (89) becomes

$$\frac{1}{c}\frac{\partial}{\partial t}(rE_r) - L^2(rE_r) - \ell(\ell+1)(rE_r) \quad , \tag{116}$$

which is consistent. The only other equation to check for consistency of the angular dependences (112) is equation (110). Since $B_r = 0$ this equation requires

$$\vec{E}_t - \vec{r} \times \vec{B}_t - \vec{r} \times L\psi - r \times (r \times \nabla\psi) - - r^2\nabla_t\psi \quad , \tag{117}$$

which agrees with equation (112). We have therefore found a consistent set of angular dependences for the case $E_r \neq 0$, $B_r = 0$. The image replacement will give consistent angular dependences for the $E_r = 0$, $B_r \neq 0$.

For the first case, $B_r = 0$, a wave equation for $\vec{B}_t = \vec{B}$ can be found by taking the time derivative of equation (109),

$$\frac{1}{c^2}\frac{B^2}{\partial t^2}\vec{rB} = - \frac{\partial}{\partial r}\frac{1}{c}\frac{\partial}{\partial t}(\vec{r} \times \vec{E}_t) + \frac{1}{r}\vec{L}\frac{1}{c}\frac{\partial}{\partial t}(rE_r)$$

Using $\vec{r}_0$ crossed with equation (110) in the first term on the right and equation (89) in the second term gives

$$\frac{1}{c^2}\frac{\partial^2}{\partial t^2}\vec{rB} = \frac{\partial^2}{\partial r^2}\vec{rB} + \frac{1}{r^2}\vec{L}(\vec{L} \cdot \vec{rB}) \quad . \tag{118}$$

A similar attempt to find an equation for $\vec{E}_t$ does not work out; E_r is not eliminated from the equation.

For the case $E_r = 0$, the image of equation (118) for $\vec{E}_t = \vec{E}$ is

$$\frac{1}{c^2}\frac{\partial^2}{\partial t^2} r\vec{E} = \frac{\partial^2}{\partial r^2} r\vec{E} + \frac{1}{r^2}\vec{L}(\vec{L}\cdot r\vec{E}) \quad . \tag{119}$$

These two sets of solutions are well known. The set with $B_r = 0$ are called transverse magnetic, or fields of electric type. Expanded in spherical harmonics, they represent the electric multipole fields. The set with $E_r = 0$ are called transverse electric, or fields of magnetic type, and the spherical harmonic expansion is in terms of magnetic multipole fields.

There are no radiating solutions that have both $E_r = 0$ and $B_r = 0$. If we assume that $E_r = 0$, then equation (89) shows that $\vec{L}\cdot\vec{B} = 0$. This is the same as $\vec{r}\cdot\nabla\times\vec{B} = 0$, or that the radial component of $\nabla\times\vec{B}$ must vanish. Therefore $\vec{B}_t$ is derivable from a potential, $\vec{B}_t = \nabla_t\psi$ for some ψ. Equation (110) then gives the angular dependence of E_t

$$r\vec{E}_t \sim \vec{r}\times\vec{B}_t \sim \vec{r}\times\nabla_t\psi \sim \vec{r}\times\nabla\psi \sim \vec{L}\psi \quad . \tag{120}$$

Therefore, if $B_r = 0$ also, equation (88) shows that

$$0 = \vec{L}\cdot\vec{E} = L^2\psi \quad . \tag{121}$$

The only solutions of this equation are independent of angles ($\ell = 0$), for which both $\vec{B}_t$ and $\vec{E}_t$ vanish since they are angular derivatives of ψ.

3.3 Extrapolation of Transverse Fields

The extrapolation of fields that satisfy equation (118) or (119) parallels that of the radial fields developed in Section 3.1. For outgoing waves define the delayed time T by equation (101). Then for transverse electric fields ($E_r = 0$), try expanding $\vec{E}$ in an inverse power series in r,

$$r\vec{E}(r, \theta, \phi, t) = \vec{F}_0(T, \theta, \phi) + \frac{1}{r}\vec{F}_1(T, \theta, \phi) + \frac{1}{r^2}\vec{F}_2(T, \theta, \phi) + \ldots \qquad (122)$$

Inserting this expansion in equation (119) and collecting coefficients of $1/r^{n+1}$ yields the recursion relation

$$2n\vec{F}_n = -\left[\vec{L}\,\vec{L}\cdot + (n-1)n\right]\int_0^t \vec{F}_{n-1}\,cdT \quad . \qquad (123)$$

Again $\vec{F}_0$ is arbitrary and all higher F_n are determined in terms of T-integrals of $\vec{F}_0$.

Suppose that $\vec{E}$ is known at some value r_1 of r for all θ, ϕ and T. Then $\vec{F}_0$ can be determined from the equation

$$\vec{F}_0(T, \theta, \phi) = r_1\vec{E}(r_1, \theta, \phi, T) - \frac{1}{r_1}\vec{F}_1(T, \theta, \phi) - \frac{1}{r_1^2}\vec{F}_2(T, \theta, \phi) - \ldots \qquad (124)$$

This equation can be integrated forward in time. If $\vec{F}_0$ is known at time T, equation (123) can then be used to find $\vec{F}_1(T + \delta T)$, then $\vec{F}_2(T + \delta T)$, etc. Then equation (124) gives $\vec{F}_0(T + \delta T)$. When $\vec{F}_0$, $\vec{F}_1$, $\vec{F}_2$, etc. have thus been found for all T, equation (122) gives $\vec{E}$ for all $r > r_1$. This process is suitable for numerical evaluation.

Analytically, the equations can be solved by iteration. The first approximation neglects all $\vec{F}_n$ except $\vec{F}_0$, which from equation (124) is

$$\vec{F}_0(T,\theta,\phi) = r_1 \vec{E}(r_1,\theta,\phi,T) \quad . \tag{125}$$

Then

$$r\vec{E}(r,\theta,\phi,T) = \vec{F}_0(\theta,\phi,T) \quad . \tag{126}$$

This is the approximation normally used in CHAP.

In the second approximation, equation (123) is used to evaluate $\vec{F}_1$ from $\vec{F}_0$, with the result

$$\vec{F}_1 = -\frac{1}{2} \vec{L} \vec{L} \cdot \int \vec{F}_0 c dT$$

$$= -\frac{1}{2} \vec{L} \vec{L} \cdot \int_0^T r_1 \vec{E}(r_1)\, c dT \quad . \tag{127}$$

This result is now put back in equation (124) to re-evaluate $\vec{F}_0$ to the second order,

$$\vec{F}_0 = r_1 \vec{E}(r_1) - \frac{1}{r_1} \vec{F}_1 \quad . \tag{128}$$

Both equations (127) and (128) are then used in equation (122) to extrapolate $r\vec{E}$. The result is

$$r\vec{E}(r) = r_1\vec{E}(r_1) - \frac{1}{r_1}\vec{F}_1 + \frac{1}{r}\vec{F}_1$$

$$= r_1\vec{E}(r_1) - \frac{1}{r_1}\left(1 - \frac{r_1}{r}\right)\vec{F}_1 \quad . \tag{129}$$

Note that the term in $\vec{F}_1$ here drops out at the matching radius $r = r_1$.

Equation (129) gives the first-order correction for diffraction that occurs in the region $r > r_1$. As seen in equation (127), the correction involves an integration of the lowest-order field in time and an application of the angular derivative operator $\vec{L}\,\vec{L}\cdot$. Higher order corrections involve repeated applications of the time integration and angular derivatives.

Let us examine the sign of the first-order correction. If $E(r_1)$ is positive at all T but returns to zero for large T, then F_1 is also positive for all T but approaches a constant for large T. Equation (129) then shows that E(r) is made less positive by the correction and acquires a negative overshoot. This behavior is sketched in figure 7. The diffraction correction is trying to make E have vanishing time integral at $r = \infty$.

The relative magnitude of the correction, for spherical harmonic ℓ is

$$\frac{\delta E}{E} \approx \left(1 - \frac{r_1}{r}\right)\ell(\ell + 1)\frac{c\tau}{r_1} \quad , \tag{130}$$

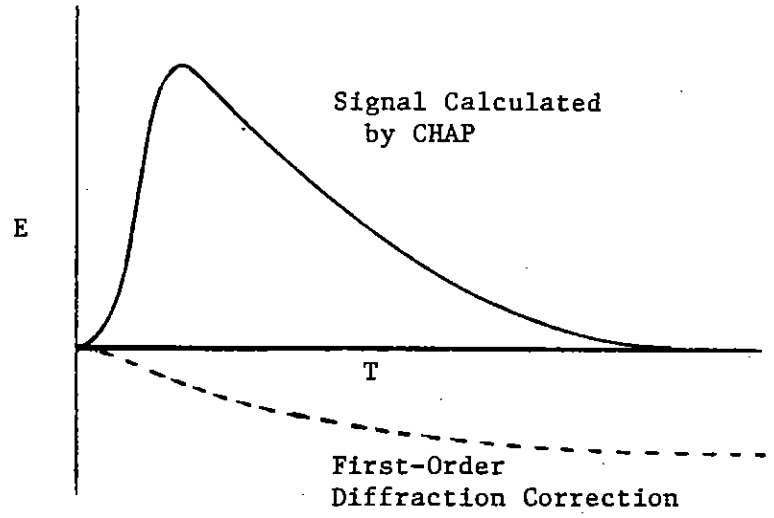

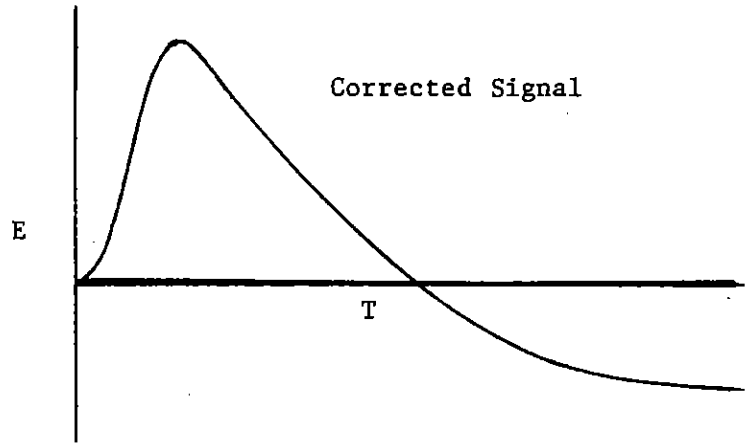

Figure 7. The effect of diffraction on the EMP calculated by CHAP, to first order. The magnitude of the correction is exaggerated in this sketch.

where τ is the pulse length at $r = r_1$. In CHAP applications, $c\tau$ is generally not larger than 100 meters, while r_1 is of the order of 100 kilometers. Thus the correction is small unless very large ℓ's are present.

While the analytical method is good for estimating the diffraction correction to the EMP during the original pulse (at $r = r_1$), it is not a convenient way to find the ultimate time wave-form of the diffracted pulse. This is best done by the numerical method, which has been applied successfully in the surface-burst EMP code LEMP. The duration of the overshoots, which make the time integral of E vanish at $r = \infty$, is of the order of r_1/c. This is much longer than the original pulse.

For transverse magnetic fields ($B_r = 0$), $\vec{E}$ in the equations of this section is replaced by $\vec{B}$. The question arises as to how to decompose an arbitrary $\vec{E}_t$ (or $\vec{B}_t$) on the surface of the sphere at $r = r_1$ into transverse electric and transverse magnetic parts.

3.4 Decomposition of Transverse Fields

Suppose we are given $\vec{E}_t$ on the surface of the sphere $r = r_1$, but have no reliable information on E_r there. (This is the situation for CHAP results.) We shall show that $\vec{E}_t$ can be decomposed into two terms

$$\vec{E}_t = \vec{L}\psi + \nabla_t \chi \quad , \tag{131}$$

where ψ and χ are two scalar functions over the surface of the sphere. First, take $\vec{L} \cdot \vec{E}_t$ and define ψ by

$$L^2\psi = \vec{L} \cdot \vec{E}_t \quad . \tag{132}$$

This equation can always be solved by expanding the scalar $\vec{L}_t \cdot \vec{E}_t$ in spherical harmonics. Then the ℓ, m harmonic part of ψ is given by

$$\psi_{\ell m} = - \frac{1}{\ell(\ell+1)} (\vec{L} \cdot \vec{E}_t)_{\ell m} \quad . \tag{133}$$

Formally, this equation can be written

$$\psi = \frac{1}{L^2} \vec{L} \cdot \vec{E}_t \quad . \tag{134}$$

Next, subtract $L\psi$ from $\vec{E}t$, defining

$$\vec{E}'_t = \vec{E}_t - \vec{L}\psi \quad . \tag{135}$$

Since $\vec{L} \cdot \vec{E}'_t = 0$, or $(\nabla \times \vec{E}')_r = 0$, the integral

$$\chi (B) = \int_A^B \vec{E}'_t \cdot d\vec{s} \quad . \tag{136}$$

between a reference point A and any other point B on the sphere surface is independent of the path taken, and therefore defines a potential function χ (B) such that

$$\vec{E}'_t = \nabla_t \chi \quad . \tag{137}$$

Equation (131) then follows. Note that $\vec{L} \cdot \nabla_t \chi = 0$ for any χ, so that the definition of ψ, equation (132) or (134), is unaffected by χ.

The function χ can be evaluated by taking the surface divergence of $\vec{E}_t$. Since $\nabla_t \cdot \vec{L}\,\psi = 0$ for any ψ

$$\nabla_t \cdot \vec{E}_t = \nabla_t \cdot \nabla\ \chi = \frac{1}{r^2} L^2\, \chi \tag{138}$$

This equation can always be solved by expanding $\nabla_t \cdot \vec{E}_t$ in spherical harmonics. Formally the solution is

$$\chi = r^2 \frac{1}{L^2} \nabla_t \cdot \vec{E}_t \quad . \tag{139}$$

From the work of Sections 3.1 and 3.2, it can be seen that $L\psi$ represents the transverse-electric part of $\vec{E}_t$, while $\nabla\chi$ is the transverse part of the electric field going with the transverse-magnetic fields. Since in the latter case we actually need the magnetic field, it is better to find χ such that

$$\chi = \frac{1}{L^2} \vec{L} \cdot \vec{B}_t \quad . \tag{140}$$

Then $\vec{L}\chi$ is the transverse-magnetic part of $\vec{B}_t$.

3.5 Application to CHAP Results

Analysis of the fields at $r = r_1$ in terms of spherical harmonics is a considerable task. Since we desire only an estimate of the effect of diffraction on the EMP calculated by CHAP for the Kingfish event, we adopt a simpler approach.

In CHAP coordinates, θ is the angle of the observer with respect to the (downward) vertical through the burst point, and ϕ is the azimuthal angle about ground zero. Because the geomagnetic field was not far from horizontal (dip angle $\approx 30°$), the electric field was principally E_θ. The most rapid variation of E_θ was with θ, rather than ϕ, because the air density varies exponentially with height or θ. This variation of E_θ with θ means that $\nabla_t \cdot \vec{E}_t \neq 0$. Thus there must be an E_r, since $\nabla \cdot \vec{E} = 0$. Therefore, we are dealing primarily with transverse-magnetic fields, and the diffraction analysis should be applied to B_ϕ and B_θ. The operator $\vec{L}$ applied to $\vec{B}$ is

$$\vec{L} \cdot \vec{B} = \frac{1}{\sin\theta} \frac{\partial}{\partial\theta} \sin\theta \, B_\phi - \frac{1}{\sin\theta} \frac{\partial}{\partial\phi} B_\theta \qquad (141)$$

Since B_ϕ is larger than B_θ and $\partial/\partial\theta$ is larger than $\partial/\partial\phi$, we may drop the last term in this equation. Then picking out the ϕ-component of $\vec{L}\,\vec{L} \cdot \vec{B}$ gives

$$L_\phi \vec{L} \cdot \vec{B} \approx \frac{\partial}{\partial\theta} \frac{1}{\sin\theta} \frac{\partial}{\partial\theta} \sin\theta \, B_\phi \quad . \qquad (142)$$

Equation (129) for the extrapolated B_ϕ then becomes

$$rB_\phi(r) = r_1 B_\phi(r_1) - \frac{1}{r_1} \left(1 - \frac{r_1}{r}\right) F_{\phi 1} \quad , \qquad (143)$$

where

$$F_{\phi 1} = -\frac{1}{2} \frac{\partial}{\partial\theta} \frac{1}{\sin\theta} \frac{\partial}{\partial\theta} \sin\theta \int_0^T r_1 \, B_\phi(r_1) \, cdT \quad . \qquad (144)$$

To apply this to CHAP, one needs to run CHAP for several rays at different θ's, running them out to an r_1 just outside the source region. Then the angular differentiation and time integration are done to find the correction factor $F_{\phi 1}$. The results of this calculation are given in the classified companion report, Reference 4. Because in CHAP B_ϕ and E_θ are very nearly equal, the correction was actually applied to E_θ.

If the fields were mostly transverse electric, the correction would have been applied chiefly to E_ϕ. The fractional correction to E_ϕ would have been about the same as that to B_ϕ or E_θ.

LIST OF REFERENCES

1. Longmire, C. L., "Close-in E. M. Effects Lectures X and XI," Los Alamos National Laboratory Report LAMS-3073, April 1964 (unpublished).

2. Karzas, W. J. and R. Latter, Phys. Rev., Vol. 137B, PG. 1369, 1965.

3. Longmire, C. L., IEEE Trans. on Ant. and Prop., Vol. AP-26, PG. 3, January 1978.

4. Hamilton, R. M., C. L. Longmire and S. R. Schwartz, "Justification and Verification of High-Altitude EMP Theory, Part II," Mission Research Corp., MRC-R-1037, Nov. 1986 (unpublished).

5. Longmire, C. L., "The Early-Time EMP from High-Altitude Nuclear Explosions, Mission Research Corp., MRC-R-809, DNA-TR-84-175, December 1983.

6. Longmire, C. L. R. M. Hamilton and J. M. Hahn, "A Nominal Set of High-Altitude EMP Environments," Mission Research Corp., Santa Barbara, Calif. MRC-R-991, 30 APRIL 1986.

APPENDIX A
FIELD RADIATED BY A SINGLE ELECTRON

The formula for the electric field radiated by a moving and accelerating electron is derived in References 7 and 8. In MKS units, the formula is

$$\vec{E}(\vec{r}_0,t_0) = \frac{Z_0}{4\pi}\frac{-e}{R}\frac{\vec{n}\times[(\vec{n}-\vec{\beta})\times\dot{\vec{\beta}}]}{(1-\vec{n}\cdot\vec{\beta})^3} \qquad \text{(A-1)}$$

Here Z_0 is the impedance of space,

$$Z_0 = 120\pi \text{ ohms (to 0.1\%)} \quad . \qquad \text{(A-2)}$$

R is the distance from the electron to the observer,

$$R = \left|\vec{r}_0 - \vec{r}(t)\right| \quad , \qquad \text{(A-3)}$$

where $\vec{r}(t)$ is the position of the electron at standard time t. The velocity of the electron at this time, divided by c, is $\vec{\beta}$ and $\dot{\vec{\beta}}$ is the time derivative of $\vec{\beta}$ at the same time. The unit vector $\vec{n}$ is in the direction of $\vec{r}_0 - \vec{r}(t)$. The field radiated by the electron at t arrives at the observer at standard time t_0,

$$t_0 = t + R/c \quad . \qquad \text{(A-4)}$$

As in Section 2.3 we assume that the electron is born at the origin t = 0, and that the observer's coordinate z_0 is very large compared with the gyro radius L. Then the variation of $\vec{n}$ over the electron trajectory is small compared with that of $\vec{\beta}$, and $\vec{n}$ can be taken as constant and in the z-direction. Further, if the right-hand side is evaluated at the delayed time T_e of the electron, it will give directly the electric field at the delayed time $T_0 = T_e$ of the observer.

Turning now to the evaluation of the vector products in equation (A-1), note that both $\vec{\beta}$ and $\dot{\vec{\beta}}$ are in the x,z plane, as is also $\vec{n}$. Therefore $(\vec{n} - \vec{\beta}) \times \dot{\vec{\beta}}$ can have only a y-component, which is

$$\begin{aligned}[(\vec{n} - \vec{\beta}) \times \dot{\vec{\beta}}]_y &= (n_z - \beta_z)\dot{\beta}_x - (n_x - \beta_x)\dot{\beta}_z \\ &= \dot{\beta}_x + \beta_x\dot{\beta}_z - \beta_z\dot{\beta}_x \\ &= \omega_e\beta[\cos\omega_e t - \beta] \quad . \end{aligned} \tag{A-5}$$

Here we have used equation (22) for β_x and β_z. Since $\vec{E}$ involves the vector product of $\vec{n}$ with this vector, $\vec{E}$ has only an x component,

$$E_x(\vec{r}_0, T_0) = \frac{Z_0}{4\pi}\frac{e\omega_e\beta}{R}\frac{(\cos\omega_e t - \beta)}{(1-\beta\cos\omega_e t)^3} \quad . \tag{A-6}$$

The relation between t and $T_0 = T_e$ is equation (32), or

$$\omega_e T_0 = \omega_e t - \beta\sin\omega_e t \quad . \tag{A-7}$$

We also show here that

$$\int_{\omega_e t=0}^{\pi} E_x(T_0)dT_0 = 0 \quad . \tag{A-8}$$

To perform this integration, it is most convenient to express dT_0 in terms of dt by equation (31), or

$$dT_0 = (1-\beta\cos\omega_e t)dt \quad . \tag{A-9}$$

Therefore the indefinite integral

$$I \equiv \int \frac{\cos\omega_e t - \beta}{(1-\beta\cos\omega_e t)^3}\,\omega_e dT_0 \tag{A-10}$$

$$= \int \frac{\cos\phi - \beta}{(1-\beta\cos\phi)^2}\,d\phi \quad , \tag{A-11}$$

where $\phi = \omega_e t$. It can be shown by differentiation that the indefinite integral is

$$I = \frac{\sin\phi}{1-\beta\cos\phi} \quad . \tag{A-12}$$

Therefore, the integral from 0 to π vanishes, as stated. Also, the integral from 0 to $\omega_e t$ is

$$I(\omega_e t) = \frac{\sin\omega_e t}{1-\beta\cos\omega_e t} \quad . \tag{A-13}$$